Chemical Science

ROYAL SOCIETY OF CHEMISTRY

EDGE ARTICLE

View Article Online
View Journal | View Issue

Cite this: *Chem. Sci.*, 2021, **12**, 9189

All publication charges for this article have been paid for by the Royal Society of Chemistry

Received 8th May 2021
Accepted 6th June 2021

DOI: 10.1039/d1sc02547c

rsc.li/chemical-science

Photoinduced 1,2-dicarbofunctionalization of alkenes with organotrifluoroborate nucleophiles *via* radical/polar crossover†

María Jesús Cabrera-Afonso, ‡[a] Anasheh Sookezian, ‡[a] Shorouk O. Badir, [a] Mirna El Khatib [b] and Gary A. Molander *[a]

Alkene 1,2-dicarbofunctionalizations are highly sought-after transformations as they enable a rapid increase of molecular complexity in one synthetic step. Traditionally, these conjunctive couplings proceed through the intermediacy of alkylmetal species susceptible to deleterious pathways including β-hydride elimination and protodemetalation. Herein, an intermolecular 1,2-dicarbofunctionalization using alkyl *N*-(acyloxy) phthalimide redox-active esters as radical progenitors and organotrifluoroborates as carbon-centered nucleophiles is reported. This redox-neutral, multicomponent reaction is postulated to proceed through photochemical radical/polar crossover to afford a key carbocation species that undergoes subsequent trapping with organoboron nucleophiles to accomplish the carboallylation, carboalkenylation, carboalkynylation, and carboarylation of alkenes with regio- and chemoselective control. The mechanistic intricacies of this difunctionalization were elucidated through Stern–Volmer quenching studies, photochemical quantum yield measurements, and trapping experiments of radical and ionic intermediates.

Introduction

The vicinal difunctionalization of alkenes has emerged as an enabling technology in organic synthesis to access diverse structural skeletons from readily available building blocks.[1,2] In particular, intermolecular 1,2-dicarbofunctionalization (DCF) reactions represent a powerful method to install two carbon subunits across an unsaturated system in one step with an accompanying increase in molecular complexity.[3] Traditionally, DCF efforts have been largely limited to transition-metal-mediated processes, with[1] or without[2] the aid of a photocatalyst (Fig. 1A). Palladium,[4] nickel,[5] copper,[6] and other metals[7] have all been utilized to afford 1,2-substituted products. Although these DCF advancements represented milestones in their own right, the necessity of a metal catalyst can lead to numerous deleterious pathways, such as β-hydride elimination, homocoupling, isomerization, or proto-demetalation.[1]

Radical/polar crossover (RPC) has recently been enlisted to assemble challenging structural motifs under mild reaction conditions (Fig. 1B).[8,9] Under RPC paradigms, odd-electron intermediates are generated through single-electron transfer (SET) and then engage in further transformations. The resulting radical species can subsequently undergo single-electron

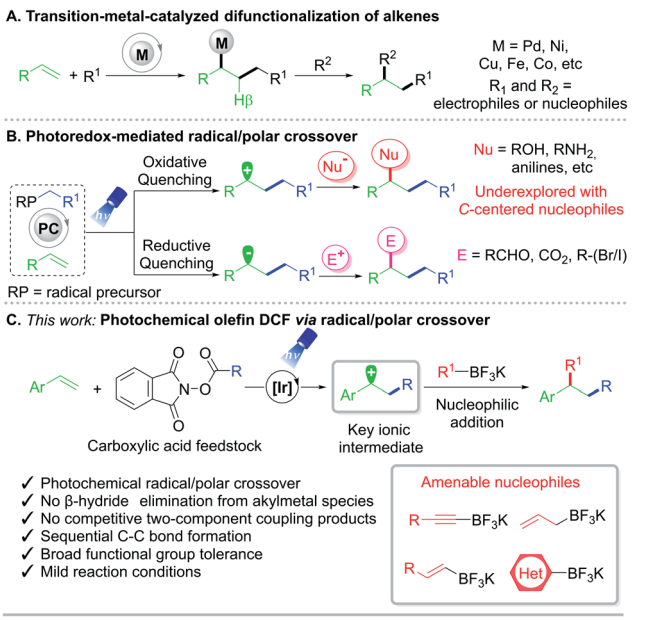

Fig. 1 Strategies for olefin 1,2-difunctionalization. (A) Transition-metal-catalyzed difunctionalizations. (B) Overview of photochemical radical/polar crossover. (C) Developed vicinal dicarbofunctionalization using organotrifluoroborate nucleophiles.

[a]*Roy and Diana Vagelos Laboratories, Department of Chemistry, University of Pennsylvania, 231 South 34th Street, Philadelphia, Pennsylvania 19104-6323, USA. E-mail: gmolandr@sas.upenn.edu*

[b]*Department of Biochemistry and Biophysics, Perelman School of Medicine, University of Pennsylvania, Stellar-Chance Building, 422 Curie Boulevard, Philadelphia, Pennsylvania 19104-6059, USA*

† Electronic supplementary information (ESI) available: Experimental and mechanistic studies details, as well as spectral data. See DOI: 10.1039/d1sc02547c

‡ These authors contributed equally.

reduction[10,11] or oxidation[12,13] to enter the two-electron reaction domain for further diversification. Although photo- and electrochemical RPC-mediated intermolecular 1,2-DCFs that proceed with *in situ* formed carbanions have been reported, these efforts are largely limited to carbonyl alkylation[8d,10] or carbocarboxylation.[8d,11]

Methods to incorporate carbon-centered nucleophiles typically rely on the use of electrophilic radicals including perfluoroalkyl feedstocks as well as strongly nucleophilic, electron-rich systems in conjunction with Lewis acids or peroxides as additives.[13] In this vein, the development of a general RPC route employing two carbon-based coupling partners for DCF remains elusive. Importantly, the implementation of a unified approach toward the carboallylation, carboalkenylation, carboalkynylation, and carboarylation of alkenes presents a formidable, yet highly powerful scenario to rapidly assemble molecular complexity from commodity chemicals.

Discussion

As part of a program centered on the development of catalytic tools for alkene functionalization, a photochemical intermolecular 1,2-dicarbofunctionalization of olefins with alkyl *N*-(acyloxy)phthalimide redox-active esters (RAEs) as radical progenitors has been developed (Fig. 1C). RAEs are bench-stable solids readily accessible from carboxylic acids with an established propensity to undergo decarboxylative fragmentation upon single-electron reduction.[14] We envisioned that radical addition to vinyl arenes would generate key radical and carbocation intermediates that could be harnessed in sequential bond formation through RPC. With these goals in mind, the interrogation of potassium organotrifluoroborates as nucleophiles to construct C–C linkages under photoredox catalysis was considered, as they have been shown to engage in addition reactions under Brønsted and Lewis acid catalysis.[15] Furthermore, alkynyltrifluoroborates have been enlisted as alternative nucleophilic partners in Suzuki–Miyaura cross-couplings, with the Bsp^3–Csp bond being adequately polarized to engender a direct transmetalation event.[16] From a synthetic standpoint and through the same RPC reactivity mode, the proposed strategy would facilitate carboallylation, carboalkenylation, carboalkynylation, and carboarylation from commodity chemicals with regio- and chemoselective control. Notably, this net-neutral photochemical RPC process is driven by SET events that occur predominantly between the photocatalyst and substrates/intermediates, bypassing the requirement for stoichiometric external reductants or oxidants.

To examine the feasibility of the proposed reaction design, 4-acetoxystyrene **1a**, aliphatic RAE **2a**, and potassium (2-phenylethynyl)trifluoroborate **3a** were employed (Table 1). A more detailed optimization of the equivalences of reaction components, catalyst loading, solvent, and reaction concentration is

Table 1 Optimization of reaction conditions[a]

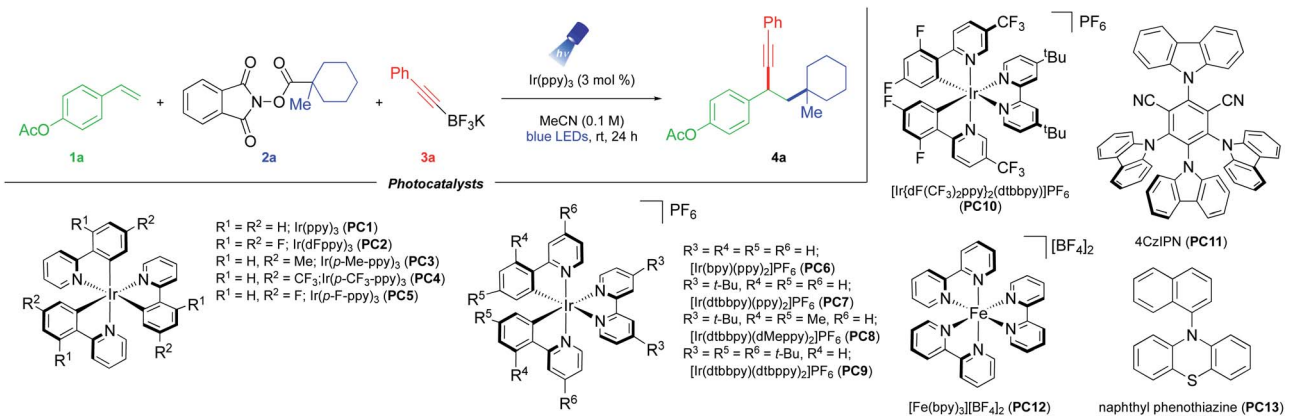

Entry	Deviation from std. conditions	% Yield[b]	Entry	Deviation from std. conditions	% Yield[b]
1	**None**	**89**	10	**PC10** instead **PC1**	nr
2	**PC2** instead **PC1**	81	11	**PC11** instead **PC1**	Trace
3	**PC3** instead **PC1**	67	12	**PC12** instead **PC1**	nr
4	**PC4** instead **PC1**	91	13	**PC13** instead **PC1**	nr
5	**PC5** instead **PC1**	89	14	20 mol% $Cu(OTf)_2$	32
6	**PC6** instead **PC1**	52	15	20 mol% $Yb(OTf)_3$	36
7	**PC7** instead **PC1**	58	16	No PC	nr
8	**PC8** instead **PC1**	68	17	No light	nr
9	**PC9** instead **PC1**	81			

[a] Reaction conditions: styrene **1a** (0.1 or 0.2 mmol), RAE **2a** (1.5 equiv.), potassium organotrifluoroborate salt **3a** (2 equiv.), $Ir(ppy)_3$ (3 mol%) in MeCN (0.1 M), 24 h irradiation with blue LEDs (λ_{max} = 456 nm). [b] Yields were determined by ^1H NMR analysis using trimethoxybenzene as internal standard. Abbreviations: std, standard; nr, no reaction.

provided in the ESI.† Here, the most relevant findings are highlighted, namely the critical performance of photoredox catalysts on the DCF outcome.

Notably, the crux of this net-neutral RPC approach is a series of well-orchestrated, single-electron oxidation and reduction steps. To achieve chemo- and regio-selectivity, the following criteria must be considered: (i) the aliphatic RAE should be more susceptible to reduction than the alkene or the resulting benzylic radical formed upon addition to the olefin. (ii) The alkyl radical should react with alkene **1** at a rate faster than its single-electron oxidation to a carbocation intermediate or radical dimerization. (iii) The rate of benzylic radical oxidation must be competitive with its addition to another equivalent of the styrene. (iv) The rate of single-electron oxidation of the benzylic radical must be faster than that of the radical intermediate generated from RAE reduction. (v) The rate of nucleophilic addition of the potassium organotrifluoroborate to the benzylic carbocation should take place preferentially over single-electron oxidation of the organoboron reagent under photoredox conditions. (vi) This rate must also be competitive with the nucleophilic addition of phthalimide anions generated upon decarboxylative fragmentation of the RAE. In this vein, the choice of photocatalyst significantly impacts product distributions. Given the propensity of RAEs to undergo SET ($E_{1/2}^{red}$ = −1.26 V *vs.* SCE for 1-methylcyclohexyl-*N*-hydroxyphthalimide-ester[17]), a palette of catalysts in acetonitrile (MeCN) was surveyed (entries 1–13). Reducing iridium-based (Ir) photocatalysts in combination with 2-phenylpyridine (ppy) derived-ligands (entries 1–9) exhibited optimal reactivity, affording **4a** in excellent yield. Importantly, in the absence of a highly oxidizing photocatalyst, the corresponding organotrifluoroborates would not undergo SET.[18] As expected, weaker reductants, **PC10** ($Ir^{IV}/*Ir^{III}$ $E_{1/2} = -1.00$ V *vs.* SCE[19]) and organic dye **PC11** ($PC^{\cdot+}/PC^*$ $E_{1/2} = -1.12$ V *vs.* SCE[19]), showed little (entry 11) to no conversion (entry 10). Notably, iron-based catalyst **PC12** ($Fe^{III}/*Fe^{II}$ $E_{1/2} = -1.65$ V *vs.* SCE[19]) and organic sensitizer **PC13** ($PC\cdot^{+}/PC^*$ $E_{1/2} = -2.1$ V *vs.* SCE[19]) resulted in full recovery of the styrene derivative (entries 12–13), presumably because they possess a short excited-state lifetime (for **PC13**, $\tau = \sim$0.8–2.3 ns (ref. 19)). Inspired by precedents on the activation of RAEs with Lewis acids,[20] the influence of these additives on the outcome of the three-component photochemical paradigm was studied. Surprisingly, the addition of $Cu(OTf)_2$ or $Yb(OTf)_3$ led to a decrease in yield (entries 14–15). Control experiments omitting light as well as photocatalyst validated the necessity of all reaction components to facilitate sequential bond formation (entries 16–17).

With suitable conditions established, the scope of RAEs with nucleophile **3a** was evaluated (Scheme 1). In general, the reaction is amenable to an array of unactivated secondary and tertiary radical architectures. The method further benefits from broad substrate tolerance, facilitating the incorporation of a strained cyclobutane subunit (**4b**), a Boc-protected amine (**4d**), a bridged bicycle (**4e**), acyclic moieties, as well as biologically relevant scaffolds including lipid-lowering agent gemfibrozil (**4h**). In addition, efficient product formation occurs in the presence of an internal olefin (**4c**), showcasing the chemoselectivity of this protocol toward styrenyl-type systems. Notably, RAE bearing a chloride handle (**4g**, **4k**, **4y**, **4ah**, **4ai**) can be introduced without compromising yields, delivering linchpins that can drive molecular complexity through subsequent transition metal-mediated functionalization.

Next, the reactivity of various potassium organotrifluoroborates using 4-acetoxystyrene **1a** was evaluated (Scheme 1). Carboallylation proved feasible, affording the difunctionalized product (**4j**) in good yield, while simultaneously incorporating an olefinic moiety that can engage in diverse downstream alkene transformations. Although progress has been made in conjunctive cross-couplings employing transition-metal catalysts with alkynyl, alkenyl, alkyl, and aryl electrophiles, the use of allyl counterparts remains scarce.[21,22] In addition to β-hydride elimination associated with alkylmetal species, these processes are further complicated by the generation of undesired two-component allylation products. Importantly, the allyl handle might be susceptible to additional insertion events resulting in oligomerization.[21,22] In this vein, the utility of the developed three-component allylation is partially driven by its ability to deliver two $C(sp^3)$–$C(sp^3)$ linkages selectively from readily available building blocks. Similarly, potassium arylethynyltrifluoroborates bearing electron-donating (*para*-methoxy, **4k**) or electron-neutral (naphthyl, **4l**) substituents serve as effective nucleophiles. The phenyl moiety was successfully replaced by primary short- (**4m**) and long-chain (**4o**) alkyl groups as well as more sterically hindered carbocycles (**4n**). The scope was further extended to alkenyltrifluoroborates (**4p–4s**), with aryl-substituted derivatives performing slightly better under the reaction conditions. Notably, both the (*E*)- and (*Z*)-isomers of 1-propenyltrifluoroborate resulted in product formation with retention of stereochemistry about the olefin (**4p**, **4q**).

Remarkably, aryltrifluoroborates function as competent nucleophiles, facilitating intermolecular 1,2-alkylarylation (Scheme 1). Substitution at the para- and meta-positions of the aryl scaffolds was explored, whereby efficient photocoupling took place. Specifically, alkoxy derivatives, a methyl thioether, and a Boc-protected amine were successfully harnessed to afford difunctionalized synthetic frameworks (**4t–4aa**). The amenability of aryltrifluoroborates provides a facile, unique approach toward the synthesis of 1,1-diaryl compounds of significance in drug discovery efforts.[23] Furthermore, medicinally relevant heterocycles such as furan (**4ab**, **4ad**) and thiophene (**4ac**) moieties exhibited good reactivity. Notably, this photoredox-mediated RPC proceeds exceptionally well with electron-rich aryl systems that suffer from lower coupling efficiency in certain transition-metal-catalyzed cross-couplings. The mild reaction conditions (room temperature, additive-free, and near-neutral pH) serve to suppress side reactivity stemming from an otherwise competitive hydrodeboration of the trifluoroborate starting material.

Finally, the scope of olefins was investigated (Scheme 1). In general, styrenes bearing no substitution, electron-donating, and electron-withdrawing groups at the *ortho*-, *meta*-, and *para*-positions exhibited comparable reactivity (**4ae–4ai**). Of note, aryl bromide **4ag** proved to be a suitable substrate with

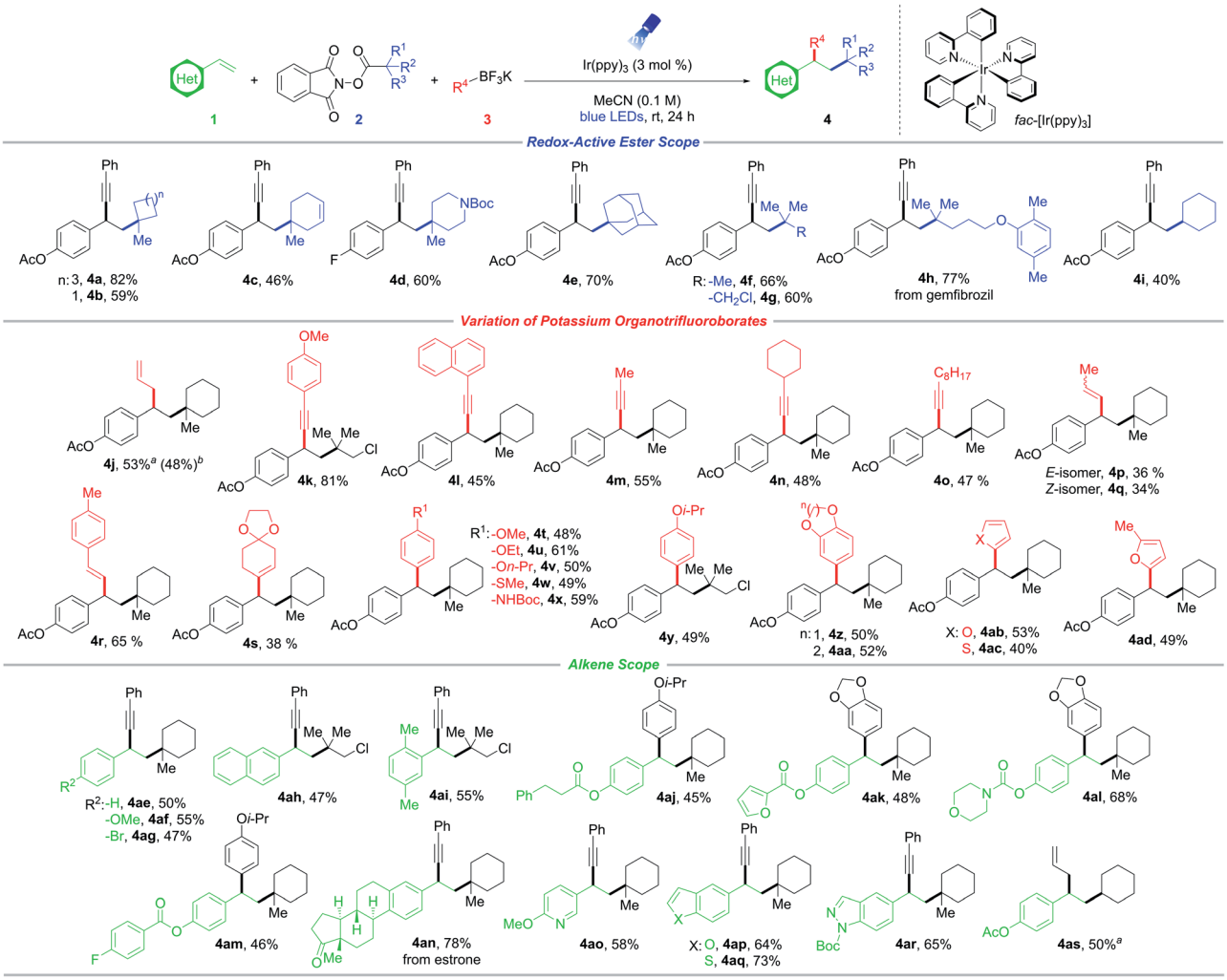

Scheme 1 Evaluation of substrate scope. Reaction conditions: styrene **1** (0.3 mmol), RAE **2** (0.45 mmol, 1.5 equiv.), potassium organotrifluoroborate salt **3** (0.6 mmol, 2 equiv.), $Ir(ppy)_3$ (3 mol%) in MeCN (3.0 mL, 0.1 M), 24 h irradiation with blue LEDs (λ_{max} = 456 nm). [a] $[Ir(dtbbpy)(ppy)_2]PF_6$ (3 mol%) was used instead $Ir(ppy)_3$. [b] Gram scale reaction: styrene **1** (6.2 mmol).

complete retention of the halide handle, providing a clear advantage in terms of scope over traditional transition-metal-catalyzed DCFs. A broad array of functional groups is tolerated, including esters, ketones, Boc-protected amines, and carbamates (**4aj–4ar**). Additionally, a substrate derived from estrone was examined, generating steroid derivative **4an** in excellent yield. Heterocyclic compounds including pyridine, benzofuran, benzothiophene, and indazole systems were readily incorporated under the developed conditions (**4ao–4ar**). In particular, these Lewis basic moieties are traditionally challenging structures in cross-couplings because of their ability to bind and poison the catalyst.

To confirm this RPC protocol was unique to potassium organotrifluoroborates, boronic acid **3xa**, pinacol boronate **3xb**, and MIDA boronate **3xc** were tested as partner nucleophiles but proved ineffectual (Scheme 2A). These results are in accordance with the *N*-parameters reported by Mayr,[24] a solvent-dependent nucleophilicity scale, which identified potassium organotrifluoroborates as one of the most reactive nucleophilic organoboron sources.

To investigate the reaction mechanism, radical and carbocation trapping studies were performed under standard conditions (Scheme 2). Addition of TEMPO (2,2,6,6-tetramethyl-1-piperidinyloxy) inhibited product generation. Specifically, recovery of 4-acetoxystyrene **1a** was observed, and the corresponding TEMPO adduct **5** was isolated and confirmed *via* NMR and HRMS analysis (Scheme 2B). To probe the intermediacy of carbocation species, nucleophilic trapping experiments were conducted using *O*-centered nucleophiles with slight modifications in the loading of these reagents (3.0 equiv. of MeOH or 30.0 equiv. of H_2O). The corresponding ether **6** and alcohol **7** were successfully isolated and characterized, providing further credence to the existence of an ionic pathway (Scheme 2C).

Stern–Volmer luminescence studies of individual reaction components established that the excited state photocatalyst was quenched most effectively by the aliphatic RAE with an observed

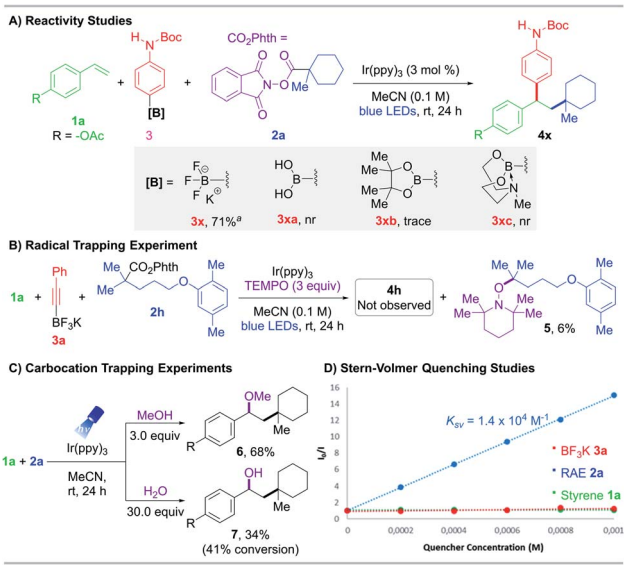

Scheme 2 (A) Reactivity studies of organoboron compounds. (B) Radical trapping experiments. (C) Carbocation trapping experiments. (D) Stern–Volmer quenching. Reaction conditions: styrene **1** (0.2 mmol), RAE **2** (0.3 mmol, 1.5 equiv.), potassium organotrifluoroborate salt **3** (0.4 mmol, 2 equiv.), $Ir(ppy)_3$ (3 mol%) in MeCN (2.0 mL, 0.1 M), 24 h irradiation with blue LEDs ($\lambda_{max} = 456$ nm). [a]Yield was determined by ^1H NMR analysis using trimethoxybenzene as internal standard. Abbreviations: nr, no reaction.

constant K_{SV} of 1.4×10^4 M^{-1} (Scheme 2D, see the ESI†). Furthermore, the photochemical quantum yield Φ of this reaction is 0.26, indicating that a radical chain mechanism is unlikely or inefficient (see the ESI†).[25]

Based on these findings, a mechanistic scenario is postulated (Scheme 3) whereby excitation of $Ir(ppy)_3$ under blue light irradiation generates a potent excited state $*[Ir]^{III}$ complex ($E_{1/2}$ $[Ir^{IV}/Ir^{*III}] = -1.88$ V *vs.* SCE[19]). Single-electron transfer (SET) to RAE **2** ($E^{red}_{1/2} = -1.26$ V *vs.* SCE for 1-methylcyclohexyl-*N*-hydroxyphthalimide ester[17]) induces formation of C(sp^3)-hybridized radical **A** followed by extrusion of carbon dioxide. Subsequent addition of this reactive intermediate to vinyl arene **1** furnishes a relatively stabilized 2° benzylic radical **B** ($E^{ox}_{1/2} = 0.37$ V *vs.* SCE[26]). Single-electron oxidation of this species by $[Ir]^{IV}$ ($E_{1/2}$ $[Ir^{IV}/Ir^{III}] = 0.77$ V *vs.* SCE[19]) yields the corresponding carbocation **C**, restoring the ground-state photocatalyst. At this critical juncture, ionic intermediate **C** is intercepted by the organotrifluoroborate nucleophile **3** to furnish the desired 1,2-dicarbofunctionalized product **4**.

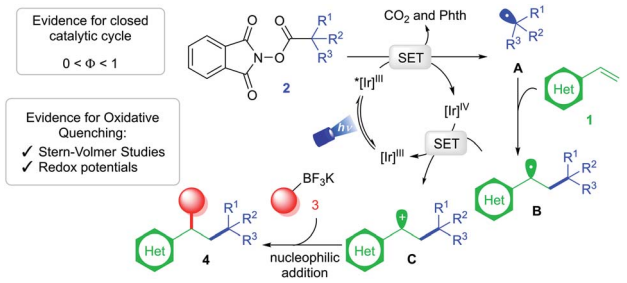

Scheme 3 Proposed mechanism of photoinduced olefin dicarbofunctionalization *via* RPC.

Conclusions

In summary, a unified protocol to achieve the carboallylation, carboalkenylation, carboalkynylation, and carboarylation of olefins with regio- and chemoselective control has been developed. Through an oxidative quenching pathway, the photoreduction of aliphatic RAEs has been enlisted to generate reactive alkyl radical intermediates that react with alkene feedstocks in a regulated fashion. The resulting *C*-centered radical undergoes single-electron oxidation to afford a key carbocation intermediate that is intercepted by organotrifluoroborate nucleophiles to facilitate sequential C–C bond formation under mild reaction conditions. Mechanistic studies, including Stern–Volmer quenching studies, photochemical quantum yield measurements, and trapping experiments of radical and ionic intermediates, emphasize that a RPC-mediated mechanism is likely operational. Most importantly, this report provides a general blueprint toward 1,2-dicarbofunctionalizations in the absence of organometal species.

Author contributions

The project was conceived by Shorouk O. Badir. Dr María Jesús Cabrera-Afonso and Shorouk O. Badir performed Stern–Volmer quenching studies. Dr Mirna El Khatib conducted quantum yield experiments. Dr María Jesús Cabrera-Afonso and Anasheh Sookezian contributed equally. Dr María Jesús Cabrera-Afonso, Anasheh Sookezian, and Shorouk O. Badir performed experiments with input from Professor Gary A. Molander. Shorouk O. Badir, Dr María Jesús Cabrera-Afonso, and Anasheh Sookezian wrote the manuscript with input from Professor Gary A. Molander.

Conflicts of interest

There are no conflicts to declare.

Acknowledgements

The authors are grateful for financial support provided by NIGMS (R35 GM 131680 to G. M.). Shorouk O. Badir is supported by the Bristol-Myers Squibb Graduate Fellowship for Synthetic Organic Chemistry. Dr María Jesús Cabrera-Afonso acknowledges the Fundación Ramón Areces for a Postgraduate Fellowship in Life and Matter Sciences. Anasheh Sookezian thanks Janssen Pharmaceuticals for financial support. Dr Mirna El Khatib is thankful for financial support provided by NHLBI (K25 HL145092-01). The NSF Major Research Instrumentation Program (award NSF CHE-1827457), the NIH supplement awards 3R01GM118510-03S1 and 3R01GM087605-06S1, as well as the Vagelos Institute for Energy Science and Technology supported the purchase of the NMRs

used in this study. We thank Dr Sergei Vinogradov (UPenn) for his input in the photochemical quantum yield measurements. Stern–Volmer measurements were conducted in the Facility for Spectroscopic Excellence (UPenn) through a collaboration with JASCO Corporation. We thank Dr Charles W. Ross, III (UPenn) for mass spectral data. Johnson Matthey is acknowledged for the donation of iridium(III) chloride, Kessil for the donation of lamps, and Frontier Scientific for the donation of organotrifluoroborates.

Notes and references

1 For selected reviews in the presence of a photocatalyst, see: (*a*) J. Li, Y. Luo, H. W. Cheo, Y. Lan and J. Wu, *Chem*, 2019, **5**, 192; (*b*) S. O. Badir and G. A. Molander, *Chem*, 2020, **6**, 1327; (*c*) C. Zhu, H. Yue, L. Chu and M. Rueping, *Chem. Sci.*, 2020, **11**, 4051.

2 For selected reviews on DCF in the absence of a photocatalyst, see: (*a*) R. K. Dhungana, S. Kc, P. Basnet and R. Giri, *Chem. Rec.*, 2018, **18**, 1314; (*b*) R. Giri and S. KC, *J. Org. Chem.*, 2018, **83**, 3013; (*c*) J. Lin, R.-J. Song, M. Hu and J.-H. Li, *Chem. Rec.*, 2019, **19**, 440.

3 For representative synthesis of bioactive compounds, see: (*a*) S. KC, P. Basnet, S. Thapa, B. Shrestha and R. Giri, *J. Org. Chem.*, 2018, **83**, 2920; (*b*) S. KC, R. K. Dhungana, V. Aryal and R. Giri, *Org. Process Res. Dev.*, 2019, **23**, 1686; (*c*) T. Yang, X. Chen, W. Rao and M. J. Koh, *Chem*, 2020, **6**, 738.

4 For representative examples using palladium, see: (*a*) M. Koy, P. Bellotti, F. Katzenburg, C. G. Daniliuc and F. Glorius, *Angew. Chem., Int. Ed.*, 2020, **59**, 2375; (*b*) M. Catellani and G. P. Chiusoli, *Tetrahedron Lett.*, 1982, **23**, 4517; (*c*) E. W. Werner, K. B. Urkalan and M. S. Sigman, *Org. Lett.*, 2010, **12**, 2848; (*d*) L. Liao, R. Jana, K. B. Urkalan and M. S. Sigman, *J. Am. Chem. Soc.*, 2011, **133**, 5784; (*e*) M. Orlandi, M. J. Hilton, E. Yamamoto, F. D. Toste and M. S. Sigman, *J. Am. Chem. Soc.*, 2017, **139**, 12688.

5 For representative examples using nickel, see: (*a*) X. Qi and T. Diao, *ACS Catal.*, 2020, **10**, 8542; (*b*) J. Derosa, O. Apolinar, T. Kang, V. T. Tran and K. M. Engle, *Chem. Sci.*, 2020, **11**, 4287; (*c*) S. KC, R. K. Dhungana, B. Shrestha, S. Thapa, N. Khanal, P. Basnet, R. W. Lebrun and R. Giri, *J. Am. Chem. Soc.*, 2018, **140**, 9801; (*d*) Q. Lin and T. Diao, *J. Am. Chem. Soc.*, 2019, **141**, 17937; (*e*) D. Anthony, Q. Lin, J. Baudet and T. Diao, *Angew. Chem., Int. Ed.*, 2019, **58**, 3198; (*f*) W. Shu, A. García-Domínguez, M. T. Quirós, R. Mondal, D. J. Cárdenas and C. Nevado, *J. Am. Chem. Soc.*, 2019, **141**, 13812; (*g*) L. Guo, H.-Y. Tu, S. Zhu and L. Chu, *Org. Lett.*, 2019, **21**, 4771; (*h*) S. -Z. Sun, Y. Duan, R. S. Mega, R. J. Somerville and R. Martin, *Angew. Chem., Int. Ed.*, 2020, **59**, 4370; (*i*) S. KC, R. K. Dhungana, N. Khanal and R. Giri, *Angew. Chem., Int. Ed.*, 2020, **59**, 8047; (*j*) R. K. Dhungana, R. R. Sapkota, L. M. Wickham, D. Niroula and R. Giri, *J. Am. Chem. Soc.*, 2020, **142**, 20930; (*k*) X. Wei, W. Shu, A. García-Domínguez, E. Merino and C. Nevado, *J. Am. Chem. Soc.*, 2020, **142**, 13515; (*l*) D. Anthony and T. Diao, *Synlett*, 2020, **31**, 1443; (*m*) L. Guo, M. Yuan, Y. Zhang, F. Wang, S. Zhu, O. Gutierrez and L. Chu, *J. Am. Chem. Soc.*, 2020, **142**, 20390.

6 For representative examples using copper, see: (*a*) Z. L. Li, G. C. Fang, Q. S. Gu and X. Y. Liu, *Chem. Soc. Rev.*, 2020, **49**, 32; (*b*) L. Wu, F. Wang, X. Wan, D. Wang, P. Chen and G. Liu, *J. Am. Chem. Soc.*, 2017, **139**, 2904; (*c*) L. Fu, S. Zhou, X. Wan, P. Chen and G. Liu, *J. Am. Chem. Soc.*, 2018, **140**, 10965; (*d*) W. Sha, L. Deng, S. Ni, H. Mei, J. Han and Y. Pan, *ACS Catal.*, 2018, **8**, 7489; (*e*) L. Wu, F. Wang, P. Chen and G. Liu, *J. Am. Chem. Soc.*, 2019, **141**, 1887; (*f*) P.-Z. Wang, Y. Gao, J. Chen, X.-D. Huan, W.-J. Xiao and J.-R. Chen, *Nat. Commun.*, 2021, **12**, 1815.

7 For representative examples using other metals, see: (*a*) L. Liu, W. Lee, M. Y. Youshaw, M. B. Geherty, P. Y. Zavalij and O. Gutierrez, *Chem. Sci.*, 2020, **11**, 8301; (*b*) J. Terao, K. Saito, S. Nii, N. Kambe and N. Sonoda, *J. Am. Chem. Soc.*, 1998, **120**, 11822; (*c*) K. Mizutani, H. Shinokubo and K. Oshima, *Org. Lett.*, 2003, **5**, 3959; (*d*) X.-H. Ouyang, R.-J. Song, M. Hu, Y. Yang and J.-H. Li, *Angew. Chem., Int. Ed.*, 2016, **55**, 3187.

8 For representative electrochemical DCF methods, see: (*a*) G. S. Sauer and S. Lin, *ACS Catal.*, 2018, **8**, 5175; (*b*) H. Mei, Z. Yin, J. Liu, H. Sun and J. Han, *Chin. J. Chem.*, 2019, **37**, 292; (*c*) J. C. Siu, N. Fu and S. Lin, *Acc. Chem. Res.*, 2020, **53**, 547; (*d*) W. Zhang and S. Lin, *J. Am. Chem. Soc.*, 2020, **142**, 20661.

9 For selected examples on photoredox-mediated RPC, see: (*a*) R. J. Wiles and G. A. Molander, *Isr. J. Chem.*, 2020, **60**, 281; (*b*) L. Pitzer, J. L. Schwarz and F. Glorius, *Chem. Sci.*, 2019, **10**, 8285.

10 Q.-F. Bao, Y. Xia, M. Li, Y.-Z. Wang and Y.-M. Liang, *Org. Lett.*, 2020, **22**, 7757.

11 For representative RPC-mediated carboxylation reactions, see: (*a*) V. R. Yatham, Y. Shen and R. Martin, *Angew. Chem., Int. Ed.*, 2017, **56**, 10915; (*b*) J. Hou, A. Ee, H. Cao, H.-W. Ong, J.-H. Xu and J. Wu, *Angew. Chem., Int. Ed.*, 2018, **57**, 17220; (*c*) B. Zhang, Y. Yi, Z.-Q. Wu, C. Chen and C. Xi, *Green Chem.*, 2020, **22**, 5961; (*d*) H. Wang, Y. Gao, C. Zhou and G. Li, *J. Am. Chem. Soc.*, 2020, **142**, 8122.

12 For selected examples using heteroatom-based nucleophiles, see: (*a*) L. Li, H. Chen, M. Meia and L. Zhou, *Chem. Commun.*, 2017, **53**, 11544; (*b*) X.-H. Ouyang, Y. Li, R.-J. Song and J.-H. Li, *Org. Lett.*, 2018, **20**, 6659; (*c*) T. Patra, P. Bellotti, F. Strieth-Kalthoff and F. Glorius, *Angew. Chem., Int. Ed.*, 2020, **59**, 3172; (*d*) E. W. Webb, J. B. Park, E. L. Cole, D. J. Donnelly, S. J. Bonacorsi, W. R. Ewing and A. G. Doyle, *J. Am. Chem. Soc.*, 2020, **142**, 9493; (*e*) S. Shibutani, K. Nagao and H. Ohmiya, *Org. Lett.*, 2021, **23**, 1798; (*f*) G. Fumagalli, S. Boyd and M. F. Greaney, *Org. Lett.*, 2013, **15**, 4398.

13 For selected RPC-mediated protocols using C-nucleophiles, see: (*a*) A. Carboni, G. Dagousset, E. Magnier and G. Masson, *Chem. Commun.*, 2014, **50**, 14197; (*b*) Y. Duan, W. Li, P. Xu, M. Zhang, Y. Cheng and C. Zhu, *Org. Chem. Front.*, 2016, **3**, 1443; (*c*) X. Wang, Y.-F. Han, X.-H. Ouyang, R.-J. Song and J.-H. Li, *Chem. Commun.*, 2019, **55**, 14637; (*d*) M. Lux and M. Klussmann, *Org. Lett.*, 2020, **22**, 3697; (*e*)

F.-D. Lu, L.-Q. Lu, G.-F. He, J.-C. Bai and W.-J. Xiao, *J. Am. Chem. Soc.*, 2021, **143**, 4168.

14 S. Murarka, *Adv. Synth. Catal.*, 2018, **360**, 1735.

15 For selected examples, see: (*a*) S. Lee and D. W. C. MacMillan, *J. Am. Chem. Soc.*, 2007, **129**, 15438; (*b*) C.-V. T. Vo, T. A. Mitchell and J. W. Bode, *J. Am. Chem. Soc.*, 2011, **133**, 14082; (*c*) A. S. Vieira, P. F. Fiorante, T. L. S. Hough, F. P. Ferreira, D. S. Lüdtke and H. A. Stefani, *Org. Lett.*, 2008, **10**, 5215; (*d*) S. Roscales and A. Csákÿ, *Chem. Commun.*, 2014, **50**, 454; (*e*) T. N. Nguyen, T. S. Nguyen and J. A. May, *Org. Lett.*, 2016, **18**, 3786; (*f*) R. William, S. Wang, A. Mallick and X.-W. Liu, *Org. Lett.*, 2016, **18**, 4458; (*g*) S. Roscales, V. Ortega and A. G. Csákÿ, *J. Org. Chem.*, 2018, **83**, 11425; (*h*) T. N. Nguyen and J. A. May, *Org. Lett.*, 2018, **20**, 3618; (*i*) S. Sundstrom, T. S. Nguyen and J. A. May, *Org. Lett.*, 2020, **22**, 1355.

16 For selected reviews, see: (*a*) G. A. Molander, *J. Org. Chem.*, 2015, **80**, 7837; (*b*) S. Roscales and A. Csákÿ, *Chem. Soc. Rev.*, 2014, **43**, 8215.

17 G. L. Lackner, K. W. Quasdorf, G. Pratsch and L. E. Overman, *J. Org. Chem.*, 2015, **80**, 6012.

18 For selected examples using organotrifluoroborates as radical precursors, see: (*a*) J. K. Matsui, D. N. Primer and G. A. Molander, *Chem. Sci.*, 2017, **8**, 3512; (*b*) J. A. Milligan, J. P. Phelan, S. O. Badir and G. A. Molander, *Angew. Chem., Int. Ed.*, 2019, **58**, 6152; (*c*) J. Yi, S. O. Badir, R. Alam and G. A. Molander, *Org. Lett.*, 2019, **21**, 4853.

19 Y. Wu, D. Kim and T. S. Teets, *Synlett*, 2021, **32**, A.

20 S. P. Pitre, T. K. Allred and L. E. Overman, *Org. Lett.*, 2021, **23**, 1103.

21 For selected Tsuji–Trost allylation reactions, see: (*a*) B. M. Trost and M. L. Crawley, *Chem. Rev.*, 2003, **103**, 2921; (*b*) J. T. Mohr and B. M. Stoltz, *Chem.–Asian J.*, 2007, **2**, 1476; (*c*) J. D. Weaver, A. Recio III, A. J. Grenning and J. A. Tunge, *Chem. Rev.*, 2011, **111**, 1846; (*d*) B. M. Trost, *Tetrahedron*, 2015, **71**, 5708; (*e*) N. A. Butt and W. Zhang, *Chem. Soc. Rev.*, 2015, **44**, 7929.

22 For selected allylation reactions, see: (*a*) A. Yanagisawa, N. Nomura, S. Habaue and H. Yamamoto, *Tetrahedron Lett.*, 1989, **30**, 6409; (*b*) N. Nomura and T. V. RajanBabu, *Tetrahedron Lett.*, 1997, **38**, 1713; (*c*) K. Lee, J. Lee and P. H. Lee, *J. Org. Chem.*, 2002, **67**, 8265; (*d*) S. Son and G. C. Fu, *J. Am. Chem. Soc.*, 2008, **130**, 2756; (*e*) Y. Sumida, S. Hayashi, K. Hirano, H. Yorimitsu and K. Oshima, *Org. Lett.*, 2008, **10**, 1629; (*f*) B. J. Stokes, S. M. Opra and M. S. Sigman, *J. Am. Chem. Soc.*, 2012, **134**, 11408; (*g*) X. Cui, S. Wang, Y. Zhang, W. Deng, Q. Qian and H. Gong, *Org. Biomol. Chem.*, 2013, **11**, 3094; (*h*) H. D. Srinivas, Q. Zhou and M. P. Watson, *Org. Lett.*, 2014, **16**, 3596; (*i*) K. Hojoh, Y. Shido, K. Nagao, S. Mori, H. Ohmiya and M. Sawamura, *Tetrahedron*, 2015, **71**, 6519; (*j*) B. Yang and Z.-X. Wang, *J. Org. Chem.*, 2017, **82**, 4542; (*k*) H. Chen, X. Jia, Y. Yu, Q. Qian and H. Gong, *Angew. Chem., Int. Ed.*, 2017, **56**, 13103; (*l*) J. L. Hofstra, A. H. Cherney, C. M. Ordner and S. E. Reisman, *J. Am. Chem. Soc.*, 2018, **140**, 139; (*m*) X.-G. Jia, P. Guo, J. Duan and X.-Z. Shu, *Chem. Sci.*, 2018, **9**, 640; (*n*) K. Semba, N. Ohta, Y. Yano and Y. Nakao, *Chem. Commun.*, 2018, **54**, 11463; (*o*) K. Semba, N. Ohta and Y. Nakao, *Org. Lett.*, 2019, **21**, 4407; (*p*) H. Li, M. Zhang, H. Mehfooz, D. Zhu, J. Zhao and Q. Zhang, *Org. Chem. Front.*, 2019, **6**, 3387; (*q*) V. T. Tran, Z. Q. Li, T. J. Gallagher, J. Derosa, P. Liu and K. M. Engle, *Angew. Chem., Int. Ed.*, 2020, **59**, 7029.

23 For selective examples, see: (*a*) D. Ameen and T. J. Snape, *MedChemComm*, 2013, **4**, 893; (*b*) X. Liu, Y. Xiao, J.-Q. Li, B. Fu and Z. Qin, *Mol. Diversity*, 2019, **23**, 809.

24 G. Berionni, B. Maji, P. Knochel and H. Mayr, *Chem. Sci.*, 2012, **3**, 878.

25 M. A. Cismesia and T. P. Yoon, *Chem. Sci.*, 2015, **6**, 5426.

26 D. D. M. Wayner, D. J. McPhee and D. Griller, *J. Am. Chem. Soc.*, 1988, **110**, 132.